The mango tree - blossom gall midge system: toward *in-silico* assessment of management practices

Isabelle Grechi[1,3], Laurie Saint Criq[1,2], Alain Ratnadass[1,3], Frédéric Normand[1,3], Christian Soria[1,3], Lucie Brustel[1], Paul Amouroux[5], Frédéric Boudon[2,4]

[1] CIRAD, UPR HortSys, F-97455 Saint-Pierre, La Réunion, France; [2] CIRAD, UMR AGAP, F-34398 Montpellier, France; [3] HortSys, Univ Montpellier, CIRAD, Montpellier, France; [4] AGAP, Univ Montpellier, CIRAD, INRA, Montpellier SupAgro, Montpellier, France; [5] Departamento de Fruticultura y Enología, Facultad de Agronomía e Ingeniería Forestal, Pontificia Universidad Católica de Chile, Santiago, Chile

Abstract

Mango (*Mangifera indica* L.), a major fruit production in tropical and subtropical regions, is facing many production constraints. Mango yield is irregular across years, fruit quality is heterogeneous at harvest, and mango tree exhibits phenological asynchronisms within and between trees that result in long periods with phenological stages susceptible to pests and diseases. Among them, the mango blossom gall midge (BGM, *Procontarinia mangiferae* Felt) is a major pest of mango which can cause significant yield losses by damaging mango inflorescences. A mango-BGM model is currently developed from experimental data. Its final objective will be *in silico* assessment of BGM management levers (e.g., manipulation of mango phenology to synchronize flowering and soil mulching during flowering, used as physical barrier to break the BGM life-cycle). The mango-BGM model simulates the dynamics of inflorescence and BGM populations of an orchard at a daily time-step during the period of mango flowering. The orchard is structured into three zones (or patches) according to applied mulching treatments. In a first approach, the model is defined at the patch scale and considers: i) age-structured inflorescence population dynamics within each patch, accounting for natural development and BGM-induced mortality of inflorescences; ii) stage-structured BGM population dynamics within each patch, differentiating the effect of mulching treatments on the BGM life-cycle for each patch; and iii) orchard colonization and movements of BGM adults between patches, both driven by inflorescence abundance in each patch. The model was parameterized from existing knowledge and experimental data collected in Reunion Island on 'Cogshall' cultivar. In a further step, virtual experiments will be performed with the model to assess the effects of management levers on mango flowering and subsequent fruit yield, according to exogenous pest pressure. The on-going modeling approach and preliminary results are presented and discussed.

Keywords: crop-pest interactions, flowering, *Mangifera indica*, population dynamics, *Procontarinia mangiferae*, Reunion Island, soil mulching

INTRODUCTION

Mango (*Mangifera indica* L.) is the fifth most produced fruit in the world. It is a popular fruit in tropical and subtropical regions, where it is mainly produced for its economic and nutritional values. However, it is facing a number of production constraints which are: i) irregular mango bearing, with alternation of high yields in the "on" years and poor yields or failure of crop in the "off" years; ii) heterogeneity of mango batches at harvest, in fruit size as well as in fruit taste quality and postharvest behavior; and iii) strong vegetative and reproductive phenological asynchronisms within and between trees. These phenological asynchronisms have agronomical and phytosanitary impacts on mango production. On the one hand, they contribute to the heterogeneity of fruit quality and maturity at harvest. On the other hand, they extend periods during which phenological stages susceptible to pests or diseases occur in the orchard, which is a major drawback to

control their populations and damages. The long duration of these susceptible stages in mango orchards contributes to maintaining high levels of pest and disease populations. Management solutions for the mango crop are required to improve fruit yield and quality, including pesticide-free technical practices aimed at controlling mango pests and diseases.

A major pest for mango orchards in Reunion Island is the mango Blossom Gall Midge (BGM, *Procontarinia mangiferae* (Felt)) (Amouroux and Normand, 2013). The mango BGM larvae specifically develop within mango inflorescences. The last instar larvae of BGM leave the inflorescences, drop to the ground and bury themselves into the soil to pupate. Then adults emerge from pupa and leave the soil. The life-cycle lasts less than one month (Prasad (1971). By damaging inflorescences, this pest can reduce fruit yield significantly. Currently, two pesticide-free BGM management levers are considered. The first lever relies on the manipulation of mango phenology to synchronize flowering at the orchard scale. Phenological asynchronisms result from the interplays between structural and temporal components of mango architectural development (Dambreville et al., 2013). The potential control of mango phenology and flowering by various cultivation practices that could modify these components, including pruning, is currently studied (Persello et al., 2017). The second lever relies on soil mulching during flowering (Brustel, 2018). Mulching is used as a physical barrier to break the BGM life-cycle, by preventing BGM larvae from burying into or adults from emerging from the soil.

Modeling is a relevant approach to address crop-pest management issues, particularly if pest population can only be estimated indirectly as for BGM. The objective of this study was to develop a mango-BGM model that explicitly integrates mango-BGM interactions and the effect of mulching, and that eventually could be used for *in silico* assessment of BGM management levers. The modeling framework is presented.

MATERIALS AND METHODS

Plant material and data collection

Data were collected during an experiment (Brustel, 2018) carried out in 2017 in a mango orchard (cv. 'Cogshall') located at the Centre of Agricultural Production and Experimentation (CPEA) at Saint-Paul, Réunion Island (20°58'S, 55°18'E, 130 m a.s.l.). Trees were planted in 2000 with a distance of 6 m between rows and 4 m between trees within a row. The orchard was about 0.33 ha in size. It was split into three zones (or patches) according to soil mulching treatments: P1) live mulching with weed cover maintained low by mechanical mowing, P2) synthetic mulching with woven plastic ground cover, and P3) live mulching with high weed cover (Fig.1). Mulching treatments were applied in June, before mango tree flowering, and were maintained until the end of flowering.

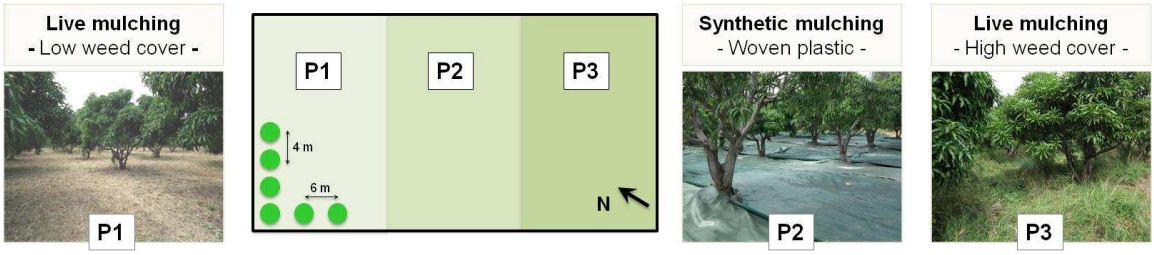

Figure1. The experimental orchard structured into three patches (P1, P2, P3) according to the soil mulching treatments.

Dataset n°1. BGM larval population was monitored from July to October with a maximum of 60 traps (i.e., two traps per tree on 10 randomly sampled trees per patch). Traps were plastic boxes with a horizontal opening of 12×12 cm and filled with water. They were installed on the ground straight under inflorescences and remained at the same position as long as inflorescences were present. When there was no longer inflorescence above, the trap was moved under new inflorescences of the same tree. If a sampled tree had no inflorescence, no trap was installed. The number of last instar larvae fallen into the traps were recorded twice a week. At the same time, the number of inflorescences above each trap

and the total number of inflorescences of each sampled tree were also recorded, enabling the number of larvae per trap to be up-scaled at the tree scale. Assuming that all the last instar larvae leaving an inflorescence located above a trap and falling to the ground were intercepted by the trap, these monitoring gave the number of last instar larvae per tree.

Dataset n°2. Flowering was monitored from July to October on 600 terminal growth units (GUs) (i.e., eight GUs per tree on 25 randomly sampled trees per patch). These trees were different from those of dataset n°1. The burst and death dates of all the inflorescences produced per GU were recorded weekly. Burst date was the date corresponding to the phenological stage C, i.e. bud opening (Dambreville et al., 2015), which is almost equivalent to stage 513 according to the BBCH scale for mango (Hernandez Delgado et al., 2011).

Modeling framework

The mango-BGM model simulates the dynamics of inflorescence and BGM populations of an orchard at a daily time-step during the period of mango flowering. In a first approach, the model is defined at the patch scale and considers: i) age-structured inflorescence population dynamics within each patch, ii) orchard colonization by exogenous BGM individuals, iii) stage-structured BGM population dynamics within each patch, and iv) movements of endogenous individuals between patches. Model inputs are the daily numbers of bursting inflorescences (i.e., those at stage C) in each of the three patches.

1. Inflorescence population dynamics

The model accounts for the natural development of inflorescences and their mortality induced by BGM larvae. Inflorescence population within a patch is age-structured, i.e. inflorescences are grouped according to their burst date. Inflorescences of age-class d are those burst at time $t = d$. Natural development of an inflorescence is assumed to last T days on average, independently on thermal time. Inflorescence lifespan can be reduced by BGM-induced mortality. Daily mortality rate of inflorescences within an age-class is assumed to be proportional to the number of larvae that have developed on those inflorescences. Finally, inflorescence population dynamics in a patch $i \in$ {P1, P2, P3} are modeled as follows:

$$I_{t,i} = \sum_d I_{t,i}^d \quad (1)$$

$$\text{with: } I_{t,i}^d = \begin{cases} B_{t,i} & \text{if } t = d \\ I_{t-1,i}^d - \min\left(1, \psi^{-1} L_{t-1,i}^d\right) I_{t-1,i}^d & \text{if } d < t < d + T \\ 0 & \text{otherwise} \end{cases}$$

where $I_{t,i}$ is the number of inflorescences at time t in the patch i, $I_{t,i}^d$ is the number of inflorescences that belong to the age-class d at time t in the patch i, $B_{t,i}$ is the number of inflorescences burst at time t in the patch i (model input), $L_{t,i}^d$ is the average number of larvae that have developed per inflorescence of age-class d from time d to t in the patch i, and ψ is a parameter representing the number of larvae required to induce inflorescence mortality.

2. BGM population dynamics

The number of BGM adult females in a patch depends on the arrival of exogenous individuals in the orchard, emergence of new individuals from soil-dwelling pupae and movement of these endogenous individuals between patches within the orchard. As the lifespan of adult females lasts only two or three days (Prasad, 1971), females egg-laying was assumed to occur during one day only. After one day, adult females were no longer considered in the model. Finally, BGM population dynamics in a patch $i \in$ {P1, P2, P3} for adult females are modeled as follows:

$$N_{t,i} = \lambda_{t,i} + \sum_{j \in \{P1,P2,P3\}} \alpha_{t,j,i} N_{t,j}^{endo} \quad (2)$$

where $N_{t,i}$ is the number of adult females at time t in the patch i, $\lambda_{t,i}$ is the number of exogenous adult females moving into the patch i at time t, $N_{t,j}^{endo}$ is the number of endogenous adult females emerging in the patch j at time t, and $\alpha_{t,j,i}$ is a parameter representing the rate of movement of endogenous individuals from the patch j to the patch i at time t.

Orchard colonization by exogenous individuals.

Based on the assumption that orchard colonization is driven by inflorescence abundance, the number of exogenous adult females moving into a patch is proportional to the number of inflorescences in this patch, such as $\lambda_{t,i} = \gamma I_{t,i}$ (3), where γ is a parameter.

Local dynamics and emergence of endogenous individuals within a patch.

The mango BGM population is stage-structured and the model accounts for BGM life-cycle within each patch (Fig. 2).

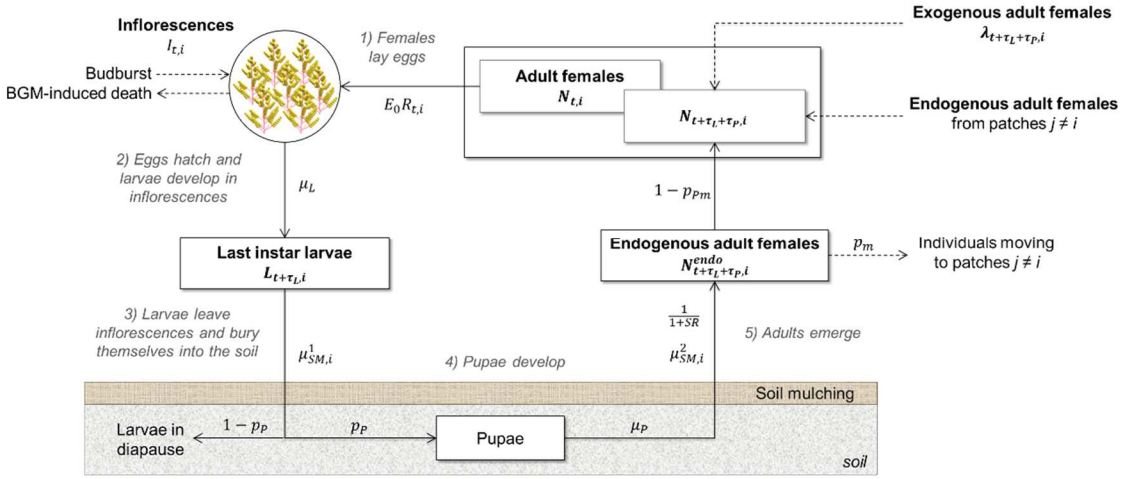

Figure 2. Schematic representation of mango BGM life-cycle and its local dynamics at the patch scale. Full-line arrows represent flux of individuals between BGM developmental stages within a patch *i*. The number of BGM individuals in a stage is the product between the number of individuals in the previous stage and the parameter(s) related to the arrow linking the two stages. Parameters are defined in Equations (4) and (5). Dashed arrows represent flux of BGM individuals between patch *i* and the outside of the patch or flux of inflorescences interacting with BGM.

Each BGM adult female can lay up to E_0 eggs on mango inflorescences. However, it is assumed that the number of eggs a female really lays depends on the amount of available resources (i.e. the number of inflorescences) per female according to a function $R_{t,i}$. It is also assumed that eggs are shared between all available inflorescences independently of their age-class. New endogenous adults emerge from soil-dwelling pupae. Some larvae do not pupate and enter in diapause up to several years. Diapausing individuals were no longer considered in the model. In addition, the model does not account for adult females emerging from larvae in diapause from previous years. The effect of mulching treatment on the BGM life cycle is differentiated for each patch. It is assumed that mulching acts as a physical barrier preventing larvae from moving into the soil and adults from emerging from the soil, partially for live mulching and totally for synthetic mulching. Finally, the local BGM population dynamics in a patch are modeled as follows:

$$N^{endo}_{t,i} = \frac{1}{1+SR}\, \mu_{SM,i}\, \mu_P\, p_P\, L_{t-\tau_P,i} \quad (4)$$

$$L_{t,i} = \mu_L\, E_0 R_{t-\tau_L,i}\, N_{t-\tau_L,i} \quad (5)$$

with: $R_{t,i} = \min\left(1, \delta \frac{I_{t,i}}{N_{t,i}}\right)$

where $L_{t,i}$ is the number of last instar larvae that drop to the ground at time t in the patch i, p_P is the proportion of larvae that pupate, τ_L and τ_P are the durations in days of larval and pupal development, μ_L and μ_P are the survival rates of eggs plus larvae and pupae, $\mu_{SM,i}$ is the product of larval ($\mu^1_{SM,i}$) and adult ($\mu^2_{SM,i}$) survival rates to mulching treatment in the patch i, SR is the sex-ratio of adult individuals, E_0 is the maximum number of eggs that a female can lay, and δ is a parameter representing the linear dependence of egg-laying regulation rate on

resource availability. As synthetic mulching is assumed to totally prevent BGM individuals from moving into or leaving the soil, $\mu_{SM,P2}$ was set to 0.

Movements of endogenous individuals between patches.

We assumed that all endogenous females remain inside the orchard and that a proportion p_m of them leaves the patch in which they have emerged to move into the other two patches. We also assumed that their movements between patches are independent of mulching treatment and are only driven by inflorescence abundance in each patch. Finally, the rate of movement of endogenous individuals from patch *j* to patch *i* at time *t*, is:

$$\alpha_{t,j,i} = \begin{cases} 1 - p_m & \text{if } i = j \\ p_m \, I_{t,i} / \sum_{k \in \{P1,P2,P3\}, k \neq j} I_{t,k} & otherwise \end{cases} \quad (6)$$

Model parameterization

Model parameters (Table 1) were either taken from the literature or estimated with experimental data. Estimations were performed sequentially. In a first step, parameters of BGM dynamics (Eq. 2-6) were estimated by setting inflorescence dynamics $I_{t,i}$, $i \in$ {P1, P2, P3}, as inputs and minimizing the following objective function:

$$f_1 = \frac{1}{3} \sum_{i \in \{P1,P2,P3\}} RMSE\left(L_{t,i}, \widehat{L_{t,i}}\right) \quad (7)$$

where $L_{t,i}$ and $\widehat{L_{t,i}}$ are respectively the observed and simulated number of the last instar larvae that drop to the ground at time t in the patch i. Values of $I_{t,i}$ and $L_{t,i}$ variables were taken from dataset n°1, by multiplying data measured at the tree scale by the number of trees per patch. In a second step, the parameter ψ accounting for BGM-induced mortality of inflorescences (Eq. 1) was estimated by using the full mango-BGM model (Eq. 1 to 6), conditionally to the parameter values estimated in the previous step, and minimizing the following objective function:

$$f_2 = \frac{1}{3} \sum_{i \in \{P1,P2,P3\}} RMSE\left(I_{t,i}, \widehat{I_{t,i}}\right) \quad (8)$$

where $I_{t,i}$ and $\widehat{I_{t,i}}$ are the observed and simulated number of inflorescences at time t in the patch i. Values of model inputs $B_{t,i}$ and the variable $I_{t,i}$ were taken from dataset n°2. As data were measured on a sub-sample of only 200 GUs, scale parameters were estimated for each patch from an independent analysis to up-scale the data to the patch scale. RMSE is the root mean squared error, a criterion used to quantify the goodness-of-fit between observed and simulated values. The smaller the RMSE is, the closer to the measurement the simulation is. In functions f_1 and f_2, RMSE was calculated on normalized values:

$$RMSE\left(Y, \hat{Y}\right) = \sqrt{\frac{1}{N} \sum_{i=1}^{N} \left(Y_i^n - \widehat{Y_i^n}\right)^2} \text{ , with: } Y_i^n = \frac{Y_i - \max(Y)}{\max(Y) - \min(Y)} \quad \text{and} \quad \widehat{Y_i^n} = \frac{\hat{Y}_i - \max(\hat{Y})}{\max(\hat{Y}) - \min(\hat{Y})}$$

The two objective functions were optimized using the basin-hopping algorithm. Basin-hopping is a stochastic and iterative algorithm which attempts to find the global minimum of a function with one or more variables (Wales and Doye, 1997). It is a two-phase method that combines a global stepping algorithm with local minimization at each step.

Model development, parameterization and simulations were performed by using Python programming language and the scipy module (Jones et al., 2001).

RESULTS AND DISCUSSION

BGM population dynamics

Using observed inflorescence dynamics as inputs, the model (Eq. 2 to 6) allowed simulating quite satisfactorily BGM dynamics in each of the three patches of the orchard. Comparison of model simulations to observed data validated, qualitatively, the ability of the model to represent the general pattern of BGM dynamics (Fig. 3). For instance, the model was able to reproduce the higher infestation level in patch P3 compared to patches P1 and P2, and the late increase of larvae number in patches P2 and P3 compared to patch P1. However, it partially failed to reproduce the high decrease of larvae number in October. It could suggest a possible seasonal pattern of orchard colonization by exogenous individuals

or individuals entering in diapause, respectively decreasing and increasing by the end of September. Observed seasonal changes in monthly diapause rate of BGM, with the lower rates occurring in winter from June to September (Amouroux et al., 2014), tend to strengthen this hypothesis.

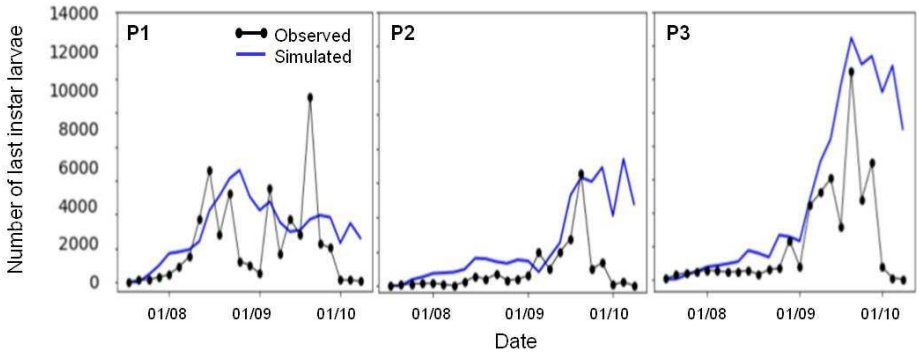

Figure 3. Observed (dataset n°1) and simulated dynamics of last instar larvae in patches P1 (low weed cover), P2 (synthetic mulching) and P3 (high weed cover).

Estimated values of model parameters (Eq. 2 to 6) are given in Table 1. These values suggest that one inflorescence attracts less than one exogenous adult female ($\gamma = 0.59$) and that about 60% of adult females emerging in a patch move to other patches ($p_m = 0.59$). They also suggest that egg-laying is maximal if there are more than 1.2 inflorescences per female ($\delta = 0.84$). Survival rate to low weed cover was very high ($\mu_{SM,P1} = 0.98$), suggesting that larvae burying into the soil and emerging adults were almost not impaired by this mulching treatment. On the contrary, less than a half of these individuals survived to high weed cover ($\mu_{SM,P3} = 0.44$). As presumed, high weed cover seems to be a more efficient mulching treatment to control BGM than low weed cover.

Table 1. Model parameters

Parameter	Unit	Eq.	Value	Source
ψ	-	(1)	102	Estimated
T	days	(1)	50	Amouroux (2013)
γ	-	(3)	0.59	Estimated
τ_L	day	(4)	7	Amouroux (2013)
τ_P	day	(5)	5	Amouroux (2013)
E_0	-	(5)	150	Amouroux (2013)
μ_L	-	(5)	0.04	Amouroux (2013)
$\mu_P p_P$	-	(4)	0.77	Amouroux et al. (2014)
$\mu_{SM,P1}$	-	(4)	0.98	Estimated
$\mu_{SM,P3}$	-	(4)	0.44	Estimated
δ	-	(5)	0.84	Estimated
SR	-	(4)	1	Amouroux (2013)
p_m	-	(6)	0.59	Estimated

Inflorescence population dynamics

Using the daily numbers of bursting inflorescences in each patch as inputs, and conditionally to the parameter values estimated for BGM dynamics, the full model (Eq. 1 to 6) allowed simulating quite satisfactorily inflorescence dynamics in two out of three patches. Comparison of model simulations to observed data validated, qualitatively, the ability of the model to represent the general pattern of inflorescence dynamics in patches P1 and P2 (Fig. 4). However, the model failed to reproduce the high number of inflorescences observed in patch P3 between September and October. The daily numbers of bursting inflorescences used as inputs were taken from a sub-sample of trees (dataset n°2) different

from the sub-sample of trees (dataset n°1) from which inflorescence and larva dynamics were derived. These two sub-samples displayed dynamics quite similar for patches P1 and P2 but very different for patch P3 (Fig. 5). This difference could partly explain why the model was not able to reproduce the inflorescence dynamics observed in patch P3.

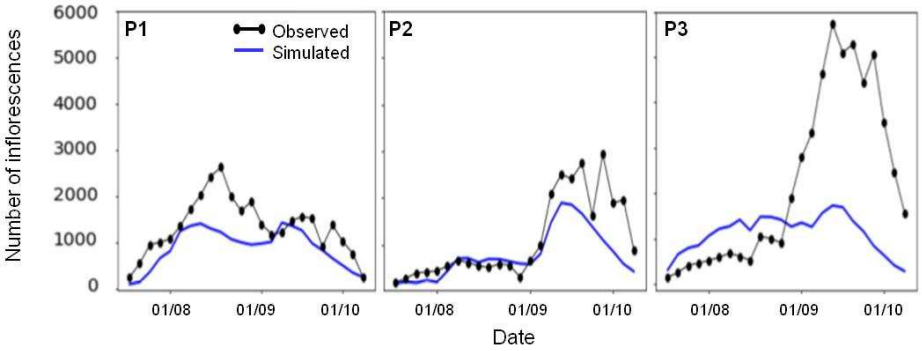

Figure 4. Observed (dataset n°1) and simulated dynamics of inflorescences in patches P1 (low weed cover), P2 (synthetic mulching) and P3 (high weed cover).

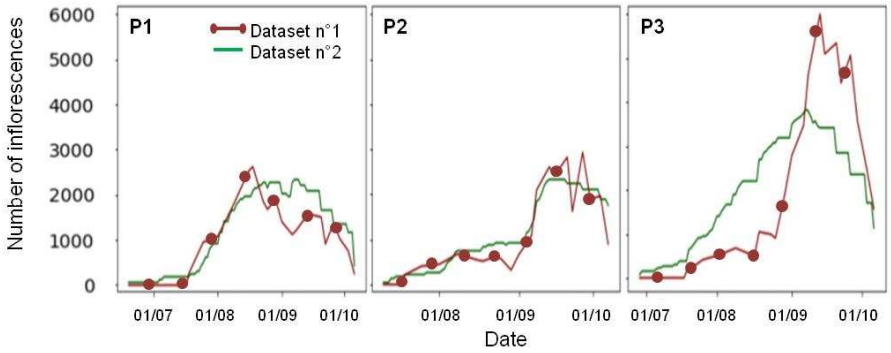

Figure 5. Observed dynamics of inflorescences in patches P1 (low weed cover), P2 (synthetic mulching) and P3 (high weed cover) according to experimental datasets.

The estimated value of the model parameter accounting for BGM-induced mortality of inflorescences (Eq. 1) is given in Table 1. This value suggests that, on average, about one hundred larvae per inflorescence are required to induce its premature mortality (ψ = 102).

From modeling to virtual experiments…

Even if the mango-BGM model was able to represent the general pattern of BGM and inflorescence dynamics, some weaknesses have been pointed out. Several improvements are needed. For instance, seasonal changes in orchard colonization by exogenous individuals and in the proportion of larvae that pupate could be investigated. One could also consider accounting for the emergence of diapausing individuals. Emergence traps could be used to measure the emergence of these diapausing individuals. In addition, as BGM dynamics were highly related to inflorescence dynamics, it seems important to calibrate the model with inflorescence and BGM data taken from a same sample of trees.

Once improved, the mango-BGM model should be used to perform virtual experiments to assess the effects of management levers on mango flowering and subsequent fruit yield, according to exogenous pest pressure. The tested environmental and management levers, and their corresponding variables or parameters, would be exogenous pest pressure (γ), mulching treatment (μ_{SM}) and manipulation of mango flowering dynamics (B_t).

CONCLUSION

This first modeling approach at the population scale gave promising results. However, further investigations are required to assess the benefits of i) considering inflorescence phenological stages, and ii) changing from a population to an individual-based and spatially explicit modeling approach, using a functional-structural plant model (FSPM) developed for

the mango tree (Boudon et al., 2017) for instance. Relying on the mango FSPM can be useful to assess the effects of pruning or other cultivation practices on mango tree flowering and their indirect effects on BGM dynamics. Eventually, the mango-BGM model could be used for the design of management solutions for a sustainable mango production, relying on a simulation-based design approach (Grechi et al., 2012).

ACKNOWLEDGEMENTS

This work has been carried out as part of the Cirad DPP COSAQ agronomical research program (activities 2016-2018) funded by European Community (FEDER working program), the Regional Council of Réunion Island and Cirad, and as part of the ECOVERGER project. This action is led by the Ministry for Agriculture and Food and the Ministry for an Ecological and Solidary Transition, with the financial support of the French Biodiversity Agency on "Resistance and Pesticides" research call, with the fees for diffuse pollution coming from the Ecophyto plan. The mango orchard was made available by the Centre of Agricultural Production and Experimentation (CPEA), whose collaboration is acknowledged.

Literature cited

Amouroux P. (2013). *Bio-écologie et dynamique des populations de cécidomyie des fleurs (Procontarinia mangiferae), un ravageur inféodé au manguier (Mangifera indica), en vue de développer une lutte intégrée*. Univ. of La Réunion, France. PhD Thesis dissertation.

Amouroux, P., and Normand, F. (2013). Survey of mango pests on Reunion Island, with a focus on pests affecting flowering. Acta Hortic. *992*, 459-466

Amouroux, P., Normand, F., Delatte, H., Roques A., and Nibouche S. (2014). Diapause incidence and duration in the pest mango blossom gall midge, *Procontarinia mangiferae* (Felt), on Reunion Island. Bull. Entomol. Res. *104(5),* 661-670.

Boudon, F., Jestin, A., Briand, A.-S., Fernique, P., Lauri, P.-É., Dambreville, A., Guédon, Y., Grechi, I., and Normand, F. (2017). The role of structural and temporal factors in the architectural development of the mango tree: evidences from simulation. Acta Hortic. *1160*, 83-90.

Brustel, L. (2018). Evaluation de l'effet de pratiques culturales (paillage / enherbement du sol / récolte prophylactique précoce) en vergers de manguier (*Mangifera indica* L.) sur la régulation de bioagresseurs de la floraison et de la fructification : les cas de la cécidomyie des fleurs (*Procontarinia mangiferae*) et des mouches des fruits (Diptera : Tephritidae). Ecole d'ingénieurs de Purpan, France. Master Thesis dissertation. https://cosaq.cirad.fr/publications/memoires-et-theses/ [Online; accessed 2018-09-26]

Dambreville, A., Lauri, P.-É., Normand, F., and Guédon, Y. (2015). Analysing growth and development of plants jointly using developmental growth stages. Ann. Bot. *115*, 93–105.

Dambreville, A., Lauri, P.-É., Trottier, C., Guédon, Y., and Normand, F. (2013). Deciphering structural and temporal interplays during the architectural development of mango trees. J. Exp. Bot. *64*, 2467-2480.

Grechi, I., Ould-Sidi, M.-M., Hilgert, N., Senoussi, R., Sauphanor, B., and Lescourret, F. (2012). Designing integrated management scenarios using simulation-based and multi-objective optimization: Application to the peach tree-*Myzus persicae* aphid system. Ecol. Model. *246*, 47-59.

Hernandez Delgado, P.M., Aranguren, M., Reig, C., Fernández Galván, D., Mesejo, C., Martínez Fuentes, A., Galán Saúco, V., and Agustí, M., (2011). Phenological growth stages of mango (*Mangifera indica* L.) according to the BBCH scale. Sci. Hort. *130,* 536–540.

Jones, E, Oliphant, E, Peterson, P, et al. (2001). SciPy: Open Source Scientific Tools for Python, http://www.scipy.org/ [Online; accessed 2018-09-26].

Persello, S., Grechi, I., Boudon, F., and Normand, F. (2017). How different pruning intensities and severities affect vegetative growth processes in 'Cogshall' mango trees. XII International Mango Symposium. 2017/07/10-16, Baise, China. https://cosaq.cirad.fr/publications/communications-a-congres/ [Online; accessed 2018-09-26]

Prasad, S.N. (1971). The mango midge pests. Cecidological Society of India, Allahabad. 172p.

Wales, D.J, and Doye, J.P.K (1997). Global optimization by basin-hopping and the lowest energy structures of Lennard-Jones clusters containing up to 110 atoms. J. Phys. Chem. A. *101(28)*, 5111-5116.